Solvent effects on the conformation of DNA dodecamer segment: A simulation study

X. Shen,[1,2] B. Gu,[3] S. A. Che,[4] and F. S. Zhang[1,2,5,a)]
[1]*The Key Laboratory of Beam Technology and Material Modification of Ministry of Education, College of Nuclear Science and Technology, Beijing Normal University, Beijing 100875, China*
[2]*Beijing Radiation Center, Beijing 100875, China*
[3]*College of Math and Physics, Nanjing University of Information Science and Technology, Nanjing 210044, China*
[4]*School of Chemistry and Chemical Technology, Shanghai Jiao Tong University, Shanghai 200240, China*
[5]*Center of Theoretical Nuclear Physics, National Laboratory of Heavy Ion Accelerator of Lanzhou, Lanzhou 730000, China*

(Received 11 December 2010; accepted 24 June 2011; published online 21 July 2011)

Different solvent temperatures with five kinds of counterions are used to investigate solvent effects on the DNA microscopic structure. The dodecamer d (CGCGAATTCGCG) DNA segment is merged into the solvents and its conformation transition is studied with the molecular dynamics simulations in detail. For the simple point charge model of water molecule with Na^+ counterions, as temperature increases from 200 K to 343 K, the duplex DNA changes from stiff B form to a state between A form and B form, which we define as mixed (A-B) structure, with a double helix unwinding. To study the counterions effects, other four alkali cations, Li^+, K^+, Rb^+, or Cs^+ ions, are substituted for Na^+ ions at 298 K and 343 K, respectively. For the cases of Li^+, Rb^+, and Cs^+ ions, the duplex DNA becomes more flexible with sugar configuration changing form C2′-*endo* to C1′-*endo* type and the width and depth of minor groove at CpG and GpC steps moving towards A values, as the mass of the counterions decreasing. For the case of K^+ ions, DNA-K^+ interaction widens the width of minor and major grooves at ApA steps and TpT steps, respectively. It seems that the light ions (Li^+ or Na^+) prefer to interact with the free phosphate oxygen atoms while the heavier ions (Rb^+ and Cs^+) strongly interact with the base pairs. © *2011 American Institute of Physics*. [doi:10.1063/1.3610549]

I. INTRODUCTION

The structure of DNA is very important in maintenance and alteration of biological inherited characters. Up to now, the subsequent DNA structure studies obtain right-handed B, A families[1] and left-handed Z helix.[2] For the B-DNA, it presents a slimmer and elongated helix with flat base pairs stacked nearly perpendicular to the helix axis. The minor groove of B-DNA is narrow and deep in contrast with a completely wide and shallow major groove. Comparing with B-DNA, the wider and stubbier A-DNA presents an empty channel in the center with the sharp cant between base pairs with the helix axis, forming a cavernous major groove and a shallow minor groove. Z-DNA is thinner and more elongated with deeper minor groove than B-DNA and completely flattened out major groove on the surface of the molecule. These DNA conformations play crucial roles in the processes of forming drug-DNA and protein-DNA complex.[3–6] There still exist broad prospects in the application of nano-biological technology of DNA devices based on their distinct conformation according to environment.[7–9] These studies help us to understand the structure-function mechanisms behind, e.g., genetic information transferring.

Many efforts have been made to study the causes of DNA conformation transitions, including internal factors and external environment sensitivities[10–13] since Watson and Crick.[14] The effect of intrinsic sequence is considered as one of the most important factors on keeping DNA conformation.[15–18] Recently, Lavery *et al.*[19] described 39 different DNA oligomers in explicit solvent and showed that sequence-effects increased at the tri- or tetranucleotide level, whereas dinucleotide models were insufficient for predicting sequence-dependent behavior. In physiological conditions, DNA conformation keeps a very delicate balance of many kinds of interactions: base stacking, backbones, hydrogen-bonds, solvent environment, etc.[20–25] Oostenbrink and van Gunsteren[26] calculated different free energy of base pairing and base stacking. Through the analysis of a diverse set of 23 natural and unnatural bases, they found stacking free energies and stacking conformations were crucial in pairing of DNA nucleotides.

In various experimental methods (x-ray crystallography, NMR and fluorescent techniques, AFM) and theoretical methods, the method of the molecular dynamics simulations has been proved to be a useful way of discovering flexibility and tracing conformation transitions at atomic level[27–32] as the complementarity to the static structure imaging techniques and the interpretation of the experiments in structure studies. Precechtelova *et al.*[33] analyzed the influence of backbone torsion angles on ^{31}P chemical shifts in DNAs with the

a)Author to whom correspondence should be addressed. Tel: +86-10-62205602. Fax: +86-10-62231765. Electronic mail: fszhang@bnu.edu.cn.

molecular dynamics simulations to overcome limitations of the static model and to obtain the geometries to construct the models. Perez *et al*.[34] presented the microsecond MD simulation of B-DNA and provided samplings that agreed well with experimental data.

As a very complicated polar solvent, with hydrogen-bond donor and acceptor, water molecules have significant effects on the properties of solutes, especially for the polymers with local partial charges. It is clear that the physiological functions of DNA molecules crucially depend on the aqueous environment.[35] However, the micro-environment of the DNA in protein binding pockets may be rather apolar.[36] Many steps in DNA isolation and preparation are carried out in apolar solvents.[37] In our previous work,[29] modified water models with scaled charges were used to study solvent polarity effects on DNA structure with the molecular dynamics simulations. As the polarity of the solvent molecule decreasing from over polarized to less polarized, DNA experienced the conformational transitions of constrained → B form → mixed (A-B) structure → A form. One of the crucial reasons for transition was considered as the competition between hydration and direct cation coupling to the free oxygen atoms of phosphate groups.

The B-DNA can be induced to the L-form duplex DNA (Ref. 38) or changes to the Z-DNA for the nucleic acids with alternation of purines and pyrimidines along one strand[39–41] when temperature is far above 298 K. Variation in temperature also leads to the melting of the DNA, which is strongly dependent on the DNA sequences, the DNA concentration, the salt concentration, ion valency, etc.[42–45] The melting temperature of the duplex d (CGCGAATTCGCG) is monitored by various techniques and it is 344.3 K in 0.1 M NaCl solution.[42] Though the stability of RNA nano-ring versus temperature has been studied recently,[46] little attention is paid to the DNA conformation transition with solvent temperature below the melting temperature, especially for the DNA, whose base sequences do not incline to form Z-DNA. The mechanisms behind the conformation transition with hydrogen-bond and ion-DNA interaction help to understand how micro-environment influences DNA conformation under intense thermal motions and why living organisms exist diversely under some extreme environments.[47]

As a highly charged polyanion, the structure and biophysical function of DNA is influenced by the cations around it.[48,49] The screening effects of counterions reduce the intramolecular repulsions generated by the charged phosphate groups and maintain structural integrity. The ions intrude into the shell of solvent molecules, replace the solvent molecules and reside there by direct or indirect contact with base pairs,[35] resulting in the changing of local DNA structure, even the conformation transition. Therefore, it is worth to study the behavior of cations or ligands around DNA and the relationship between DNA conformation changing and ionic environments.[13,45,50–54] Lyubartsev and Laaksonen[55] found that different monovalent ions interacted with DNA with very different behaviors and the different those behaviors of the ions were explained by the hydration structure around DNA. However, as far as we know, there are few studies about the counterions effects on the DNA segment at higher temperature as some intermediate states appearing in the transition process. These studies can become the useful complements for the experiments focusing on ions-DNA interactions under extreme environments.

Based on our previous work,[29] in this paper, we construct various systems as temperature ranging from 200 K to 343 K with Na^+ counterions, then substituting four kinds of alkali metal ions (Li^+, K^+, Rb^+, Cs^+) for Na^+ at 298 K and 343 K, to study solvent environment effects on the duplex d(CGCGAATTCGCG) with the intensive molecular dynamics simulations. As temperature rising up, the DNA changes from constrained to flexible B form, then stabilizing with a mixed (A-B) structure at 343 K with a double helix unwinding at the peripheries. For the alkali metal counterions, DNA conformations maintain the B form at 298 K. However, when the solvent temperature reaches 343 K, the DNA becomes more and more flexible as the mass number decreases. Different ions enter into the shell of water molecules around the free phosphate oxygen atoms and the grooves at different sites with clearly local DNA conformation changing.

After the introduction, we explain the model of water molecule, the DNA segment and ions and the simulation methods in Sec. II. The phenomena about DNA conformation transition are shown and the underlying causes of these phenomena are discussed in Sec. III with two parts: temperature effects and counterions effects. The conclusion is presented at the end of the paper.

II. MODEL AND METHODS

The NMR structure of a synthetic B form dodecamer named 171d is chosen from Protein Data Bank (PDB)[56] as the starting structure in each simulation. The 171d duplex d (CGCGAATTCGCG) is extensively studied because of its biological importance. It contains the recognition site of the *Eco*RI restriction enzyme and is frequently used in gene recombination techniques. The counterions force field parameters are present in Table I where ε and σ are Lennard-Jones parameters and model solvent is derived from the widely used flexible simple point charge (SPC) water molecule model.

The intermolecular energy consists of two parts: $E = E_{LJ} + E_C$, where E_{LJ} is the Lennard-Jones interaction and E_C is the electrostatic interaction. They are expressed as

$$E_{LJ} = 4\varepsilon_{ij}\left[\left(\frac{\sigma_{ij}}{r_{ij}}\right)^{12} - \left(\frac{\sigma_{ij}}{r_{ij}}\right)^{6}\right], \tag{1}$$

$$E_C = \frac{q_i q_j}{4\pi\varepsilon_0 r_{ij}}, \tag{2}$$

where ϵ_0 is the vacuum permittivity and r_{ij} presents the distance between two atoms. In Lennard-Jones interaction,

TABLE I. The force field parameters of alkaline metal ions.

	Li^+	Na^+	K^+	Rb^+	Cs^+
σ/Å	2.37	2.73	3.36	3.57	3.92
ϵ/kJmol^{-1}	0.149	0.358	0.568	1.602	2.132

the first term is the short-range repulsion for molecules or atoms being too close to each other, and the attraction owing to the dispersion forces is described in the second term. The Coulomb interactions between point charges describe the effects of hydrogen-bond and give the local orientational structure.[57,58] The flexibility of SPC model is considered with a Morse type of potential for its covalent bonds:[59] $V_{bond} = D(1 - exp(-\rho(r - r_{eq})))$, which is not included in Eq. (1). Here r is the distance between atoms, r_{eq} is the equilibrium bond distance, D is the well depth taken from experimentally determined dissociation energy of the O-H bond, and ρ controls the "width" of the potential.

In our simulations, the force field of Cornell *et al.*,[60] with the following functional form which we assume that readers are familiar with

$$V = \sum_{covalent\ bonds} K_b(r_b - r_0)^2 + \sum_{covalent\ angles} K_a(\theta_b - \theta_0)^2 + \sum_{torsional\ angles} \frac{1}{2}K_t(1 + \cos(m_t\phi - \phi_0)) + \sum_{i<j}\left\{4\varepsilon_{ij}\left[\left(\frac{\sigma_{ij}}{r_{ij}}\right)^{12} - \left(\frac{\sigma_{ij}}{r_{ij}}\right)^{6}\right] + \frac{q_i q_j}{4\pi\varepsilon_0 r_{ij}}\right\}, \quad (3)$$

is implemented with AMBER 94 parameters,[60] including hydrogen-bonds between base pairs, for their special accuracy in reflecting the effects of water activity.[61]

The package we use to perform molecular dynamics is M.DynaMix, which is developed for simulations of arbitrary mixtures of molecules and macromolecules in solutions.[62,63] The double time-step algorithm by Tuckerman *et al.* is implemented[64] and short time step is 0.2 fs for the fast nearest short-range (within 5Å) interactions, while the long time step for those more slowly fluctuating interaction is 2.0 fs. The cutoff for long-rang interaction R_{cut} is 14 Å. The Ewald method is adopt to treat the electrostatic interactions with screening parameter α taken as $\alpha = 3/R_{cut}$ and the reciprocal space cutoff determined[65] by $exp(-\pi^2 k_{max}^2/\alpha^2) = exp(-9)$.

In our simulation, there are one 171d DNA segment, 22 alkali metal counterions, and 4050 solvent molecules in each periodic rectangular cell ($48 \times 48 \times 56$ Å^3 at 298 K, big enough to ensure the DNA does not interact with its periodic images). At the beginning, DNA is fixed in the box center along Z direction, and a 100 ps NVT simulation is performed to allow solvent molecules and ions to form the outer shells around DNA obtaining a initial balance. Then, all of freedom degrees are released in a following 1 ns NVT running for equilibrium. After that, the product simulations of 40 ns are carried out for statistical analyses.

Structure parameters describing the global, backbone, local base pair, and groove characters of DNA are analyzed by the program Curves.[66] A local or base pair coordinate is set to quantify inter-base or intra-base parameters in a right-handed orthogonal axial set. The length (Len) of DNA and the sugar pucker phase angle (Phi) are basic characteristic distinguish A- and B-DNA. The X displacement (Xdp) describes the displacement of a base pair along the X direction (the direction of the short axis of the base pair) of the base pair axis. Inclination (Inc) is defined as dihedral angle between the base pairs and the plane with the initial x and y axis. Slide (Dy) and roll (ρ) are relative translation along the y axis and rotation around the y axis between two successive base pairs in an overall helix axis, respectively.[67] The width (MW for major groove and mW for minor groove) and depth (MD for major groove and mD for minor groove) of the groove are defined in Ref. 59. All of these parameters are analyzed continually for the precise values in our simulations.

III. RESULTS AND DISCUSSION

A. Temperature effects

To study the temperature effects on DNA conformation, the duplex DNA is put into the SPC model solvent with Na^+ counterions by changing temperature from 200 K to 343 K (set as 200 K, 260 K, 298 K, 310 K, and 343 K, respectively). The highest simulation temperature is chosen as 343 K, very close to the melting temperature (343.3 K) of 171d, which is assumed the same as the melting temperature of the duplex d (CGCGAATTCGCG) in 0.1 M NaCl solution of Ref. 42.

The strength of hydrogen-bond influences the local structure order of water and the local structure order is sensitive to the strength of dipole interaction. This order can be presented with the tetrahedral parameter

$$\langle q \rangle = \sum_{i}^{N} 1 - \sum_{j<k}^{6} \frac{3}{8}\left[\cos\theta_{ijk} + \frac{1}{3}\right]^2 \Big/ N, \quad (4)$$

which shows how nearly the nearest four neighbors of one molecule form a regular tetrahedron.[58,68] As listed in Table II, $\langle q \rangle$ decreases monotonically from 0.696 to 0.509 with temperature increasing from 200 K to 343 K. This means the local arrangement of the solvent molecules changes from tetrahedral structure to structureless random orientation. At 298 K, the tetrahedral parameter is 0.571, similar with our previous result.[29] When T=200 K, the solvent is glass-like and its local structure is fixed for the strengthened interactions. At 260 K, the fixed structure of solvent becomes flexible with $\langle q \rangle$ decreasing to 0.616. For high temperature solvent, $\langle q \rangle$ is 0.566 at 310 K, near to that of normal liquid water and its local structure still resembles a dynamical tetrahedron. However, the solvent is close to Lennard-Jones liquid with less evident local order when temperature reaches 343 K.[68] Thus the solvent changes from glass-like state to water-like solvent with flexible tetrahedral local order, then to orderless Lennard-Jones liquid, as the temperature of solvent increases from 200 K to 343 K.

TABLE II. The local tetrahedral order of the solvent structure $\langle q \rangle$ as a function of temperature.

T/K	200	260	298	310	343
$\langle q \rangle$	0.696	0.616	0.571	0.566	0.509

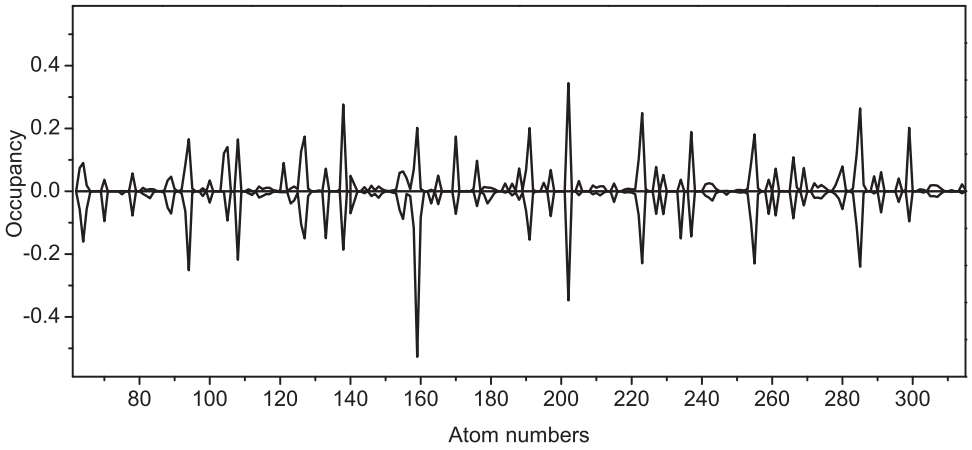

FIG. 1. Average ion occupancies for Na^+ ions with each DNA atom of inner eight base pairs along the two strands d (CGCGAATTCGCG) from 5′ to 3′ at 343 K. Occupancies with one strand atoms are present in positive values at y direction and occupancies for the other strand are present in negative values.

The ion convergence on DNA can be examined with ion occupancies between ions with the atoms of the DNA. Occupancy here is defined as the integration of the first maximum of the corresponding radial distribution function within the first shell of solvent. Fig. 1 shows Na^+ ions occupancies by atoms of inner eight base pairs in the strands form 5' to 3' at 343 K. For one strand the values are plotted at positive direction, for another strand the values are plotted at negative direction. Though the perfect symmetry with respect to the horizontal is not achieved, the palindromic symmetry is also appeared to some extent in the 40 ns trajectory. Deducing from the extent of mirror image symmetry plotted, the ion movements have mainly converged in the simulations.[13,69] It seems that ions convergence is speeded up at 343 K than that at room temperature.[13]

The root mean square coordinate deviation (RMSD) of the DNA trajectories with respect to canonical B, canonical A, and the starting PDB structure are given at 200 K, 298 K, and 343 K in Fig. 2, respectively. Here, RMSD is defined as $\Delta R_i = \sqrt{\frac{1}{N}\sum_{j=0}^{N}(\vec{r}_{ij} - \vec{r}_{ij0})^2}$, ($i$=A, B forms and the starting PDB structure), N is the number of atoms of the DNA, r_{j0} is the position of r_j in A, B form or the starting PDB structure. When temperature is 298 K, RMSD with respect to the B form fluctuates around 2.5 Å, which means no evident conformation transition from B form appears. In case of 200 K, DNA almost keeps the same conformation with the starting PDB structure under the restriction of the surrounding glass-like solvent. The corresponding RMSD is less than 2 Å and the fluctuation is less than 0.15. RMSD with respect to the B form is similar with that at 298 K but fluctuation is much smaller. Obvious change comes out when temperature rises to 343 K, the conformation deviates more than 4 Å from both B and A form after 5 ns with relatively stable mean value and the intensely violent fluctuations. Stereo views of the starting and averaged DNA structures during the last 35 ns are shown in Fig. 3. It shows that the duplex DNA changes little until the temperature rises to 343 K. Comparing with the other cases, the helix in the case of 343 K is untwined more obviously at G-C pairs than that at A-T pairs. The residual twists of the backbone mainly exist at the A-tract. The G-C pairs at the ends are broken for decreased H-bond strength of solvent molecules (see Table II) and increased thermal motions.

For the inner eight base pairs, the DNA appears the characteristics of the A form at the peripheries of duplex at 343 K. In Fig. 4, mW is more than 8.0 Å and mD is less than 3.3 Å at CpG steps, which is close to A values. However, the minor groove at A-T pairs keeps the B form with width narrower than 6.8 Å and depth deeper than 5.0 Å. As

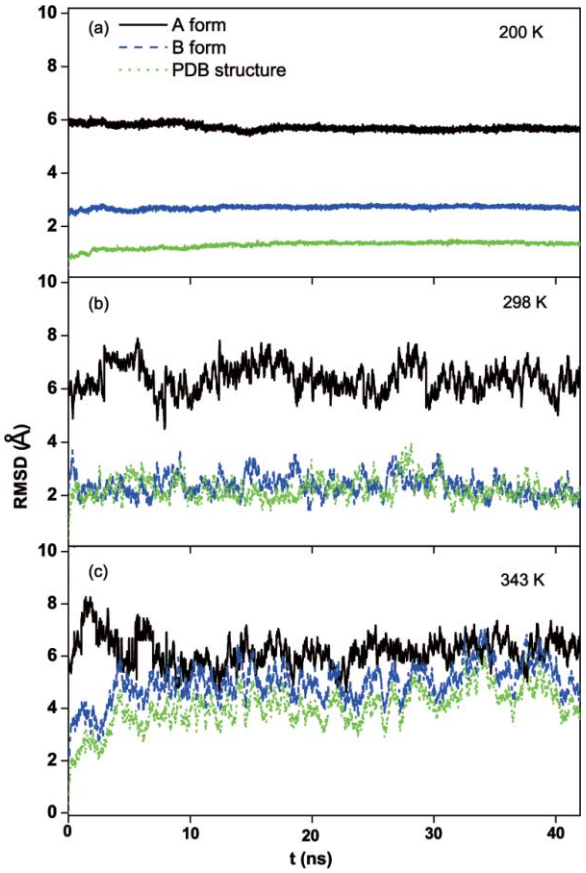

FIG. 2. RMSD of the DNA trajectories with respect to the canonical B (blue or dark gray), A forms (black), and the starting PDB structure (green or light gray).

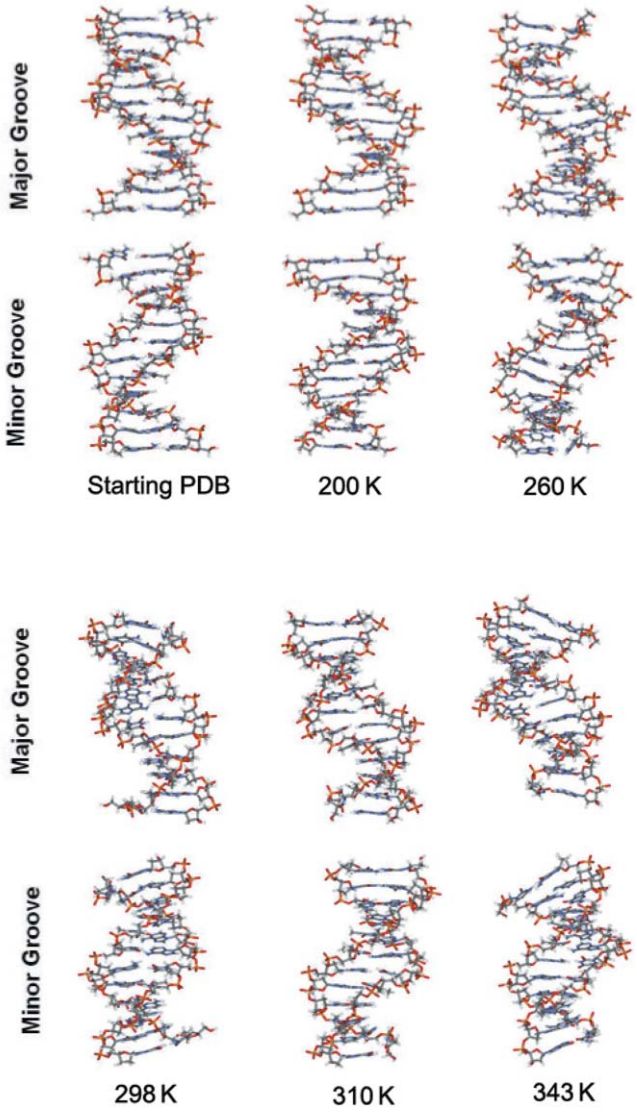

FIG. 3. Stereo views of the starting PDB structure and the generated configurations in different temperatures.

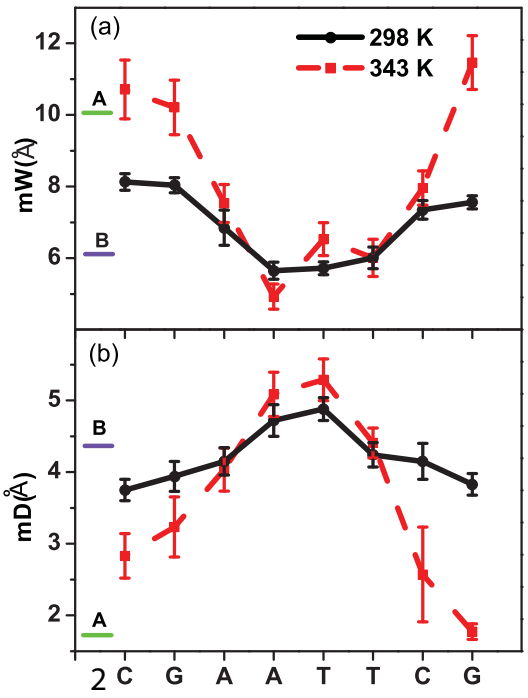

FIG. 4. The width (a) and depth (b) of minor groove of dodecamer with Na^+ counterions at 298 K and 343 K. The green (light gray) and violet (dark gray) short lines present the values of typical A and B forms, respectively.

Fig. 4 shown, mW and mD maintain B values in A-tract at 298 K, similar with the values at 343 K, but they maintain stability for the whole strands. These phenomena tell us that the solvent temperature is crucial for the duplex DNA keeping its conformation. In addition, with more consecutive stacking interaction, the inner pairs are more stable than the outer ones, although the numbers of hydrogen-bonds between A-T pair (two hydrogen-bonds) are less than that between G-C pair (three hydrogen-bonds).

To evaluate the DNA conformation transition in detail, ten distinct structure parameters are calculated. Their average values of inner eight base pairs are presented in Fig. 5. To avoid the thermal fluctuation of instantaneous conformation, we analyze 3000 average structures of every 10 ps during the last 30 ns simulations. At 298 K, all of parameters keep close to B values. For low temperature solvents, when T=200 K, all of parameters are close to the values of starting PDB structure for the duplex DNA constrained in the glass-like solvent except the parameter Inc. It maintains far above the starting PDB structure value (−6.03°) with −12.46°. At 260 K, some parameters start to change towards B values. Inc and ρ decrease to −2.1° and 1.75°, respectively. Meanwhile, Dy and MD increase to -0.70 Å and 4.85 Å, respectively. However, the other parameters nearly remain the values at 200 K. For high temperature solvents, Inc, Xdp, ρ, and MD start to change and remove steeply from B value to the middle area between A and B values at 310 K. Inc, ρ and MD increase from −3.56°, 2.05°, and 5.04 Å to 1.66°, 3.79° and 6.10 Å, respectively. Xdp decreases from −1.21 Å to −1.70 Å. At 343 K, all of parameters locate in the middle area between A and B values except MW, which is 13.67 Å, close to B value. These phenomena indicate that preferred DNA structure changes to the state between A and B form. We define this DNA state as mixed (A-B) structure, in the typical Lennard-Jones liquid as solvent temperature rising up to 343 K.

The ten structure parameters averaged over the first 10 ns are also compared with an average over the last 30 ns in Table III. Comparing with the short time simulations, most of the structure parameters do not change significantly in the last 30 ns and have mainly converged in the first 10 ns. Few differences (exceeding 5% for T < 343 K and 10% for T = 343 K) can be easily listed out. Parameter Inc deviates most from −0.21° to −3.56° at 298 K (Inc298). Beside Inc298, Inc310, Inc343, Xdp343, mD343, and MD310 are the other parameters deviating significantly and four of them appear at T > 298 K. It can be concluded that the structure converges much faster than the ion motions[13] and the violent thermal motions at high temperature influence the convergence of structure parameters obviously.

It is considered that the solvent activity determines the conformation of right-handed DNA segment, B form at high water activity, A form at reduced levels,[70] and mixed (A-B)

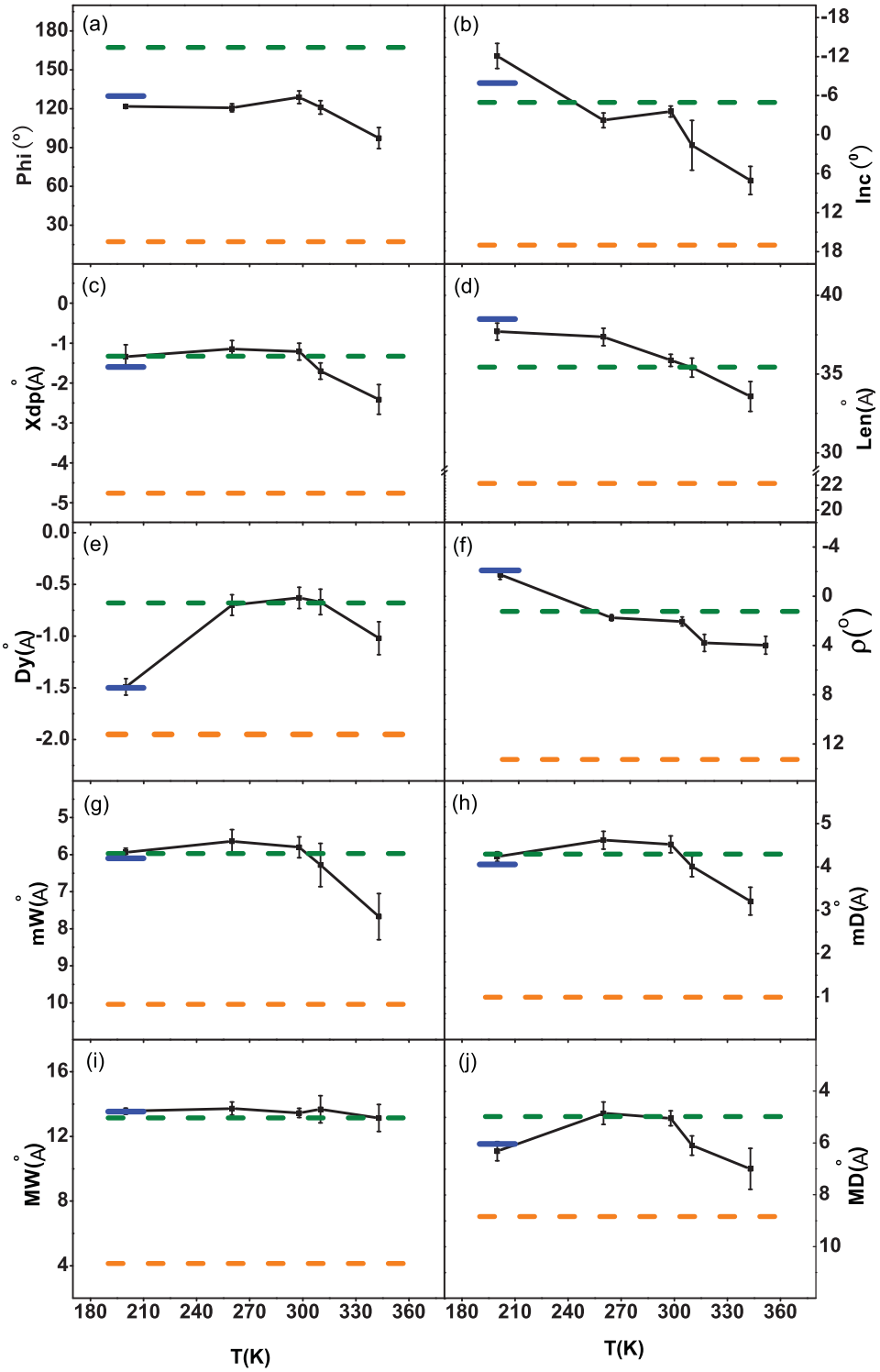

FIG. 5. Ten structure parameters at different temperatures. (a) to (f) are sugar pucker angle (Phi), inclination angle (Inc), the X-displacement (Xdp), end-to-end length (Len), slide (Dy), and roll (ρ), (g) to (j) show parameters of minor (mW and mD) and major (MW and MD) groove. The horizontal dashed lines indicate the reference values of typical A (orange or light gray) and B (cyan or dark gray) forms and the short line gives the parameters of the starting PDB structure.

structure under the mildest conditions.[71] The screening of repulsion between the negatively charged phosphate groups is considered as one of the most concerned factors for the repulsion unwinding and extending the helix without screen.[36,72] To check the underlying causes of the structural transitions induced by temperature effects, the hydration and counterions distributions around the negatively charged oxygen atoms of phosphate groups are calculated. The radial distribution functions (RDF) $g(r)_{Na^+}$ and $g(r)_{H_2O}$ are shown in Fig. 6. On one hand, when temperature increases from 298 K to 343 K or decreases from 298 K to 200 K, the first peak of $g(r)_{Na^+}$ increases from 8.86 to 13.14 or to 15.05, respectively. It shows that Na^+ ions coupling to the free oxygen atoms ($Na^+ - O^-$(P) interaction) is more and more strongly as temperature

TABLE III. The comparison of the structure parameters between the average results over the first 10 ns and the average over the last 30 ns (in brackets) at different temperatures.

T/K	200	260	298	310	343
Phi/°	120.47 (121.05)	126.39 (120.98)	124.37 (125.86)	116.82 (118.34)	106.47 (99.57)
Inc/°	− 13.02 (−12.46)	− 2.13 (−2.20)	− 0.21 (−3.56)	2.39 (1.66)	7.83 (7.08)
Xdp/Å	− 1.39 (−1.41)	− 1.11 (−1.14)	− 1.16 (−1.21)	− 1.81 (−1.75)	− 2.21 (−2.43)
Len/Å	37.54 (37.92)	37.03 (37.34)	35.70 (35.86)	35.25 (35.39)	32.98 (33.56)
Dy/Å	− 1.48 (−1.42)	− 0.74 (−0.70)	− 0.68 (−0.66)	− 0.65 (−0.67)	− 1.18 (−1.09)
ρ/°	− 1.84 (−1.79)	1.69 (1.75)	1.98 (2.05)	3.65 (3.79)	4.12 (3.98)
mW/Å	6.24 (6.23)	5.79 (5.64)	5.92 (5.80)	6.23 (6.28)	7.90 (7.67)
mD/Å	4.28 (4.25)	4.56(4.61)	4.36(4.52)	4.21(4.05)	3.03(3.37)
MW/Å	13.26 (13.11)	13.45(13.72)	13.52(13.45)	13.53(13.67)	12.86(13.13)
MD/Å	7.03 (6.78)	4.58(4.75)	5.27(5.04)	5.83(6.10)	6.92(7.00)

becoming higher or becoming lower. On the other hand, the first peak of $g(r)_{H_2O}$ decreases slightly (from 3.92 to 2.56) when temperature rises up from 200 K to 343 K. In the insets of Figs. 6(a) and 6(b), the maximum of $g(r)_{Na^+}$ decreases as the function of simulation time at 298 K while the maximum of $g(r)_{Na^+}$ increases at 343 K. Both of them converge after 20 ns with the values keeping around 13.2 and 8.80 at 343 K and 298 K, respectively.

At 298 K, the free phosphate oxygen atoms are shielded mainly by solvent molecules through hydrogen-bond. There is no evident formation of strong $Na^+-O^-(P)$ interaction which is considered as another mechanism to restrain the electrostatic repulsion on DNA backbone.[29] When T=200 K, in the insufficient sampling of the glass-like state, $g(r)_{Na^+}$ and $g(r)_{H_2O}$ present the sharpest peaks. Though the solvent molecules strongly interact with the free phosphate oxygen atoms, Na^+ ions can not be dispersed out easily for the lack of flow-ability. The cases at 260 K and 310 K are similar with that at 298 K, the counterions are dispersed out and the positively charged protons in first hydration shell shield free phosphate oxygen atoms. When T = 343 K, both the hydrogen-bond and counterions coupling are affected by thermal motions. The solvent molecules are unable to completely shield the free phosphate oxygen atoms for the decreasing hydrogen-bond and give Na^+ ions the chance to enter into the first shell of the solvent and replace the positively charged protons to interact with oxygen atoms, reflecting with a higher first peak of $g(r)_{Na^+}$ than that at 310 K or 298 K. The contributions of both counterions coupling and hydrogen-bond reach the balance at 343 K, and the mixed (A-B) structure appears. Comparing with the appearance of A form in solvent of less molecular polarity discussed in our previous work,[29] although the strength of hydrogen-bond decreases while counterions coupling keeps increasing at 343 K, the short compacted A form does not present because of the lack of effective screening of the repulsion between neighboring free oxygens on the backbone of DNA.

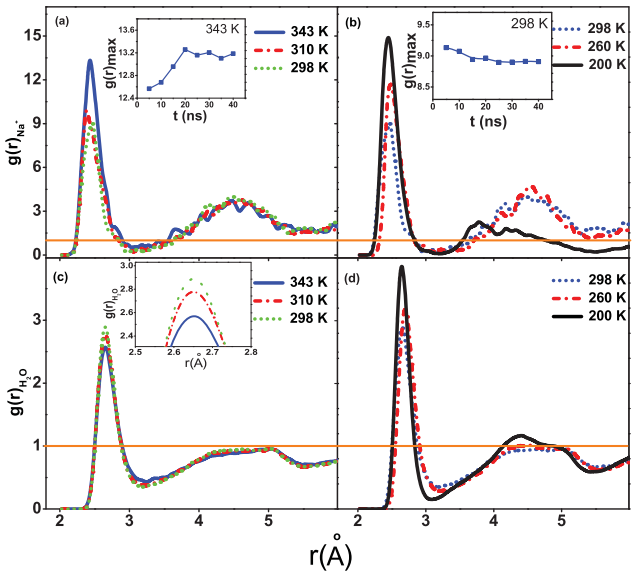

FIG. 6. Radial distribution functions (RDFs) of Na^+ ions (a), (b) and H_2O molecules (c), (d) around oxygen atoms of the phosphate groups on DNA backbones. The insets in (a) and (b) are maximums of the first peak of $g(r)_{Na^+}$ as the function of simulation time at 343 K and 298 K, respectively. The inset in (c) is the local enlarging of $g(r)_{H_2O}$.

The coordination numbers (abbreviated as CN) of Na^+ ions and the solvent molecules around the negatively charged oxygen atoms of phosphate groups are presented in Table IV. The CN here are the integration of corresponding RDF within 3 Å (RDFs are shown in Fig. 6). As the temperature increases from 200 K to 343 K, CN_{H_2O} decreases monotonically from 5.006 to 4.672 while CN_{Na^+} increases when T > 298 K or T < 298 K. At 298 K, CN_{Na^+} is only 0.260 and CN_{H_2O} is 4.786. Whereas for the low mobility of ions in glass-like solvent, Na^+ ions and solvent molecules are constrained at 200 K with the largest CN_{Na^+} (0.529) and CN_{H_2O} (5.006). The CN_{H_2O} and CN_{Na^+} at 260 K and 310 K are similar with that at 298 K except CN_{Na^+} at 260 K. It is much larger than CN_{Na^+} at

TABLE IV. Coordination numbers of Na^+ ions and H_2O around the backbone at different temperatures.

T/K	200	260	298	310	343
Na^+	0.529	0.392	0.260	0.271	0.436
H_2O	5.006	4.883	4.786	4.750	4.672

TABLE V. Diffusion coefficient ($D/10^{-9}m^2/s$) of Na^+ ions and H_2O around the backbone at different temperatures.

T/K	200	260	298	310	343
Na^+	0.005	0.392	1.469	1.471	2.813
H_2O	0.011	0.762	1.675	2.448	5.489

298 K, reaching 0.392. At 343 K, CN_{Na^+} and CN_{H_2O} reach 0.436 and 4.672, respectively. It indicates that both Na^+ ions and solvent molecules interact with the free phosphate oxygen atoms unstably.

This phenomenon can be further traced from variation of self-diffusion coefficient (D) of Na^+ ions and the solvent molecules around the backbone.[73] As Table V shown, D_{H_2O} and D_{Na^+} increase monotonically with temperature. D_{Na^+} and D_{H_2O} are $1.469\times10^{-9}m^2/s$ and $1.675\times10^{-9}m^2/s$ at 298 K, respectively, similar with our previous calculation.[29] Na^+ ions and solvent molecules are constrained at 200 K reflecting on the smallest D_{Na^+} ($0.005\times10^{-9}m^2/s$) and D_{H_2O} ($0.011\times10^{-9}m^2/s$). At 343 K, D_{Na^+} and D_{H_2O} increase to $2.813\times10^{-9}m^2/s$ and $5.489\times10^{-9}m^2/s$, respectively. This indicates that both the counterions coupling and hydrogen-bond contribute to neutralize the free oxygen on the backbones.

B. Counterions effects

To address the effects of alkali metal cations in the process of DNA conformation changing, Na^+ ions are replaced by Li^+, K^+, Rb^+, and Cs^+ ions, respectively, as the counterions in the SPC water solvent at both 298 K and 343 K.

The torsion angle of $C5'$, $C4'$, $C3'$, and $O3'$, named δ, which identifies the sugar pucker and the conformation of the deoxyribose ring, and χ, the glycosyl torsion angle between sugar and base ($O1'-C1'-N9-C4$ for purines and $O1'-C1'-N1-C2$ for pyrimidines),[74] are particularly informative. Fig. 7 shows the plot of δ as a function of χ for inner eight base pairs with different counterions. The inner base pairs are numbered with 1-8 for one strand and 9-16 for the complementary from 5′ to 3′. Sugar in B form almost presents C2′-*endo* type, δ and χ distribute in a broad range with δ ranging from 120° to 160°, and χ from −120° to −80°. C1′-*endo* is considered as an intermediate type often appearing in the sugars of mixed (A-B) structure. Whereas for the C3'-*endo* sugars of A form, δ and χ are limited around 80° and −160°, respectively.

In Fig. 7, most of plots (δ, χ) locate in the range of B value and δ and χ are linearly correlated in each figure at 298 K. Furthermore, two members of a base pair adopt configurations follow the principle of anti-correlation[75–77] for all kinds of cations. It means that different alkali metal counterions have no distinct effects on the sugar configurations under room temperature. At 343 K, ten C1′-*endo* sugars appear and four sugars are close to C3'-*endo* in case of Li^+. For K^+ ion solution, just three sugars appear C1′-*endo* and the sugars in the cases of Rb^+ and Cs^+ almost keep stable with C2′-*endo* type. It is hard to observe the correlation and anti-correlation rules between δ and χ in these four cases at 343 K. All of these phenomena indicate that the sugar in Li^+ ion solutions changes from the configuration typically appearing in B-form to the one appearing in mixed (A-B) structure. But the sugar configurations change over all base pairs instead of changing from the peripheries. In heavy ion (Rb^+ or Cs^+ ions) solutions, the plots of sugars are similar with that at 298 K, mainly maintaining C2′-*endo* type and few C1′-*endo* and C3′-*endo* types. It indicates that the sugar of B-DNA becomes more flexible in light cation solutions than that in heavier ones at a high temperature.

The same clear differences between Li^+ ions and K^+, Rb^+ and Cs^+ with the free phosphate oxygen atoms are also seen from the RDFs. In Fig. 8, as mass number increasing from Li^+ to Cs^+ ions, the first peak of $g(r)_{X^+}$ decreases from 13.20 to 7.35 when $T = 298$ K. At 343 K (Fig. 8(b)), the first peak of $g(r)_{Li^+}$ exceeds 23 while other $g(r)_{X^+}$s maintain the same maximums. It seems as the temperature rises up, Li^+ ions contact more tightly with the free phosphate oxygen atoms, resulting in the changing of sugar configurations form C2′-*endo* to C1′-*endo*, even the C3′-*endo* type. For other ion solutions (K^+, Rb^+ and Cs^+), $X^+-O^-(P)$ ("X" for different ions) interactions change little and almost all sugars maintain C2′-*endo* type.

As discussed above, DNA global structure is affected by counterions and temperature effects. Here, we go further to study the ion effects on the grooves of the duplex DNA at 343 K. Fig. 9 shows mW_X, mD_X, MW_X, and MD_X values of inner eight base pairs in different ion solutions at 343 K, respectively. The inset average widths and depths of groove demonstrate that B-DNA in light ion (Li^+ or K^+) solutions is flexible to change to mixed (A-B) structure but more stiff in heavier ones (Rb^+ or Cs^+). The line shape of mW_X in Fig. 9(a) is similar with that of mW_{Na^+}, A value (exceeding 10.0 Å) for the case of Li^+ ions and values of mixed (A-B) structure for the cases of Rb^+ and Cs^+ ions at the peripheries and typical B value in the A-tract (between 6.0 Å and 8.0 Å) of the duplex DNA as mass number increasing, except the line of mW_{K^+}. K^+-DNA interaction influences mW_{K^+} in an extraordinary approach, which has been discussed before.[35,78,79] Varnai and Zakrzewska[78] studied the behaviors of Na^+ and K^+ ions around duplex d(CCATGCGCTGAC) and found the preferred binding sites of Na^+ ion were in minor groove and K^+ ions prefer to reside in major groove. However, the condition here is slightly different. The mW_{K^+} is wider (8.0 Å) at ApA steps and narrower at TpT steps around 6.2 Å and it does not fluctuate violently at A-tract. In Fig. 9(b), the line shape of mD_{Li^+} is similar with that of mD_{Na^+}, A values at the peripheries and B values at A-tract while mD_{K^+} keeps around 3.8 Å, close to B value. For the heavier ion solutions, mD_{Rb^+} and mD_{Cs^+} maintain B value in the middle part of the duplex DNA while CpG and GpC steps locate around 2.5 Å with respect to the area of mixed (A-B) structure.

MW_X and MD_X in Figs. 9(c) and 9(d) are a bit more complicated. The average MW_Xs are not calculated because

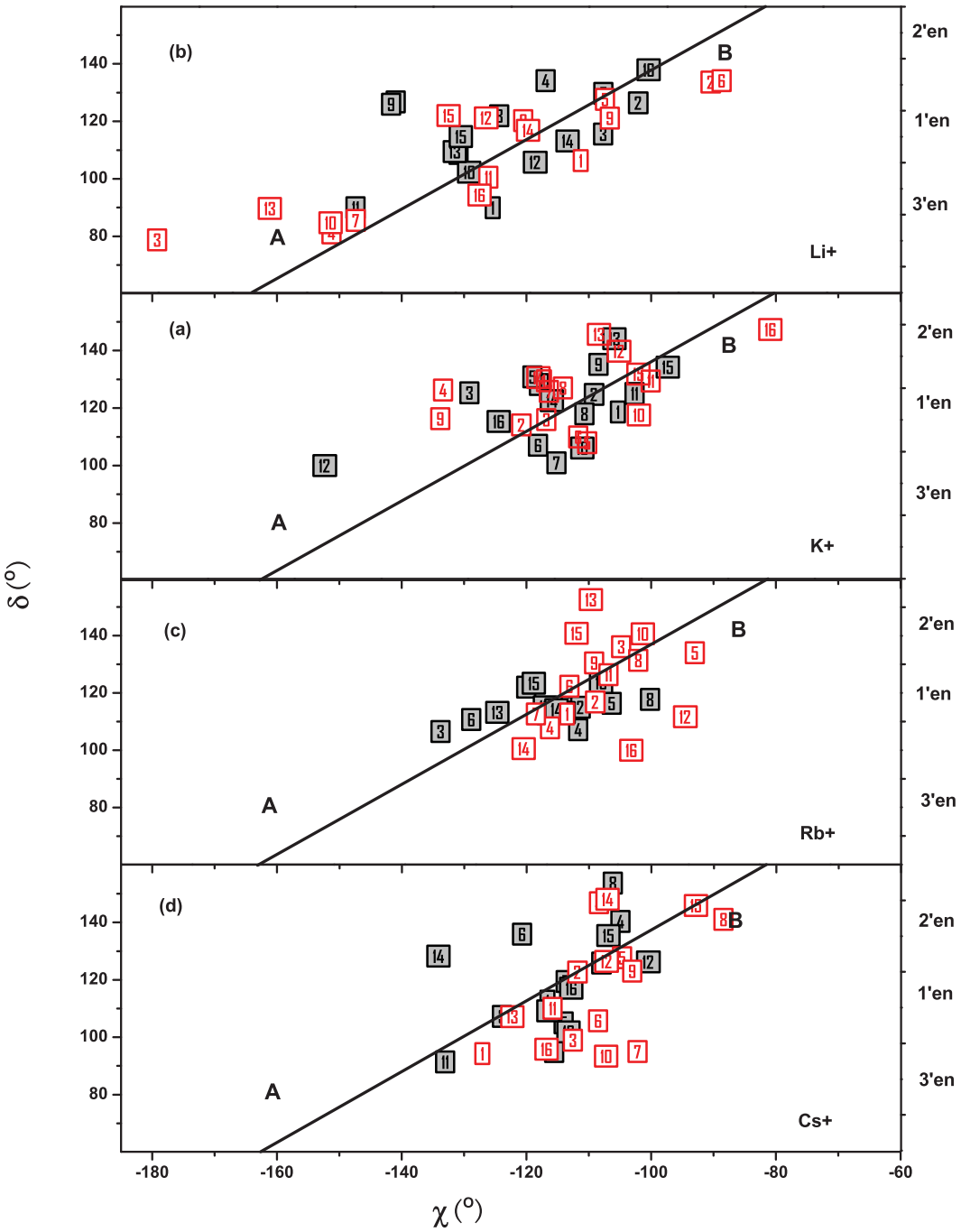

FIG. 7. Conformation plots for δ as a function of χ at 298 K and 343 K with different counterions. Bases are marked with 1-8 and 9-16 from 5' to 3' direction as dark gray squares at 298 K and red or light gray squares at 343 K. The lines in the figures present the linear correlation between δ and χ for B-DNA.

MW_Xs keep around B value in all cases between 12.0 Å and 16.0 Å. Nevertheless, an extraordinary shape of mW_{K^+} makes us concern more on the characteristics of MW_{K^+}. It seems that both mW_{K^+} and MW_{K^+} change as little as that at A-tract. In detail, mW_{K^+} is 6.4 Å averaged over ApA steps and 7.8 Å over TpT steps, while 12.0 Å averaged over TpT steps and 14.6 Å over ApA steps for the MW_{K^+}, forming a kind of complementation of the width at A-tract. In Fig. 10(d), MD_{Li^+} and MD_{K^+} are about 7.5 Å in the area between A and B values, except a gently narrowing (6.3 Å) of MD_{Li^+} at TpT steps. However, MD_{Rb^+} and MD_{Cs^+} are much shallower at GpC and CpG steps, even the protuberant groove (a negative MD)[59] appears in MD_{Cs^+}.

To sum up, Li^+ and Na^+ ions influence the grooves of DNA with a similar way, while the interaction of Rb^+ and Cs^+ ions influence the grooves of DNA with another way. The grooves in case of K^+ ions are plotted in the area of mixed (A-B) structure with not violent fluctuations except MW_{K^+}.

Counterions distributions around base pairs are calculated to discovery the underly causes between these significantly different ways. Fig. 10 shows the RDFs of cations

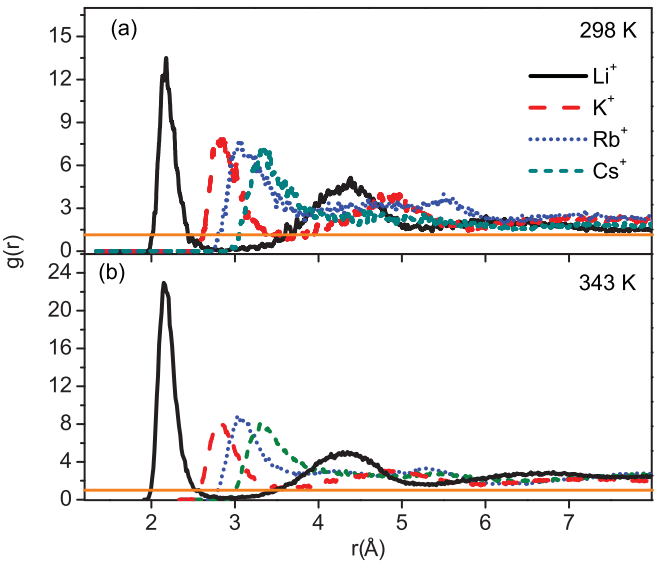

FIG. 8. RDFs of four ions around free phosphate oxygen atoms on the DNA backbones at two temperature. (a) ions-O^--(P) at 298 K. (b) ions-O^--(P) at 343 K.

around eight negative charged atoms. In Figs. 10(a)–10(d), the first peak of $g(r)_{Li^+-TO2}$ (RDF of Li^+ ions with O2 of thymine) reaches 87 at 2.4 Å. This indicates that Li^+ ions is strongly coordinated to TO2. Still the position of the first peak of $g(r)_{Li^+-GN3}$ (RDF of Li^+ ions with N3 of guanine) is beyond 5.0 Å, which means that the Li^+ ions prefer to locate at the lip of the minor groove[80] at G-C pairs and interact with the base pairs through hydration instead of entering into the minor groove. Drawing an inference from Figs. 9(a) and 9(b), mW_{Li^+} and mD_{Li^+} maintain B and A values at the strongest and the weakest interaction sites, respectively. K^+ ions have a fairly close relationship with O2 of cytosine (CO2) that the first peak of $g(r)_{K^+}$ exceeds 4 at 2.9 Å. Comparing with that of CO2, the interactions with TO2 and N3 of adenine (AN3) are relatively weak that the first peaks of $g(r)_{K^+}$ are about 1.4 at 2.8 Å and 2.1 at 2.9 Å, respectively. It can be deduced that K^+ ions contact with CO2 and GN3, forming direct DNA-K^+ interaction at G-C pairs, but few ions can intrude into the first shell of "spine of hydration." Unlike the relationship between DNA-Li^+ interaction with mW_{Li^+} and mD_{Li^+} (keeping B values at the strongest interaction sites), the strongest DNA-K^+ interaction at CO2 widens mW_{K^+} and narrows mD_{K^+}. Furthermore, the maximums of mW_{K^+} appear at the ApA steps instead of the strongest interaction sites (CpG steps). The first peaks of $g(r)_{Rb^+}$ and $g(r)_{Cs^+}$ exceed 5 around 3.5 Å in all four RDFs (Figs. 10(a)–10(d)), suggesting Rb^+ and Cs^+ ions are involved in direct interactions around all the sites in minor groove. Corresponding to mW_{Rb^+} and mW_{Cs^+} in Fig. 9, the minimum widths of the minor groove appear at the A-tract keeping B value and at the peripheries with the value of mixed (A-B) structure, respectively.

Figs. 10(e)–10(h) show the RDFs of cations with the negative charged atoms in the major groove. Li^+ ions enter into the major groove at A-tract (Fig. 10(e)) and strongly interact with AN7 that the first peak of $g(r)_{Li^+-AN7}$ reaches 18 at 2.3 Å. But there is no evident relation between $g(r)_{Li^+}$ with MW_{Li^+} and MD_{Li^+}. For K^+ ions, the direct K^+-DNA

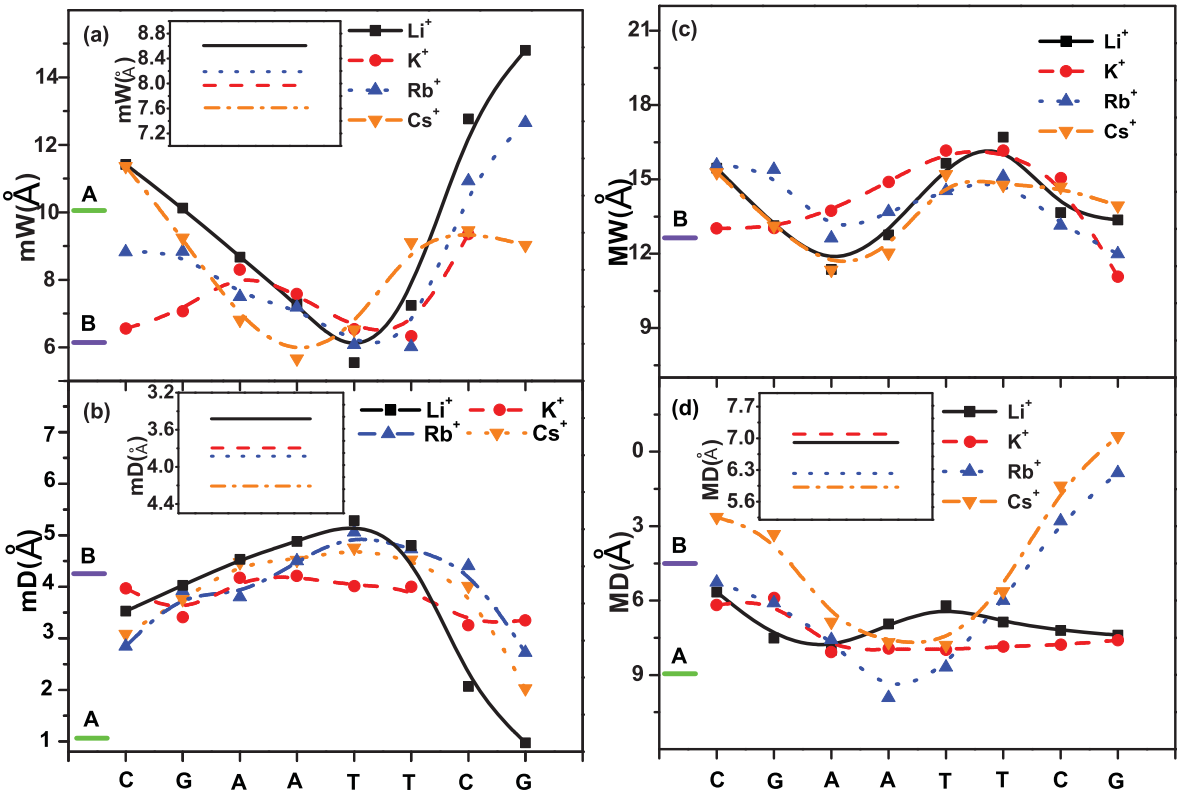

FIG. 9. The width and depth of the minor and major grooves at 343 K for different cations. The insets are the average values.

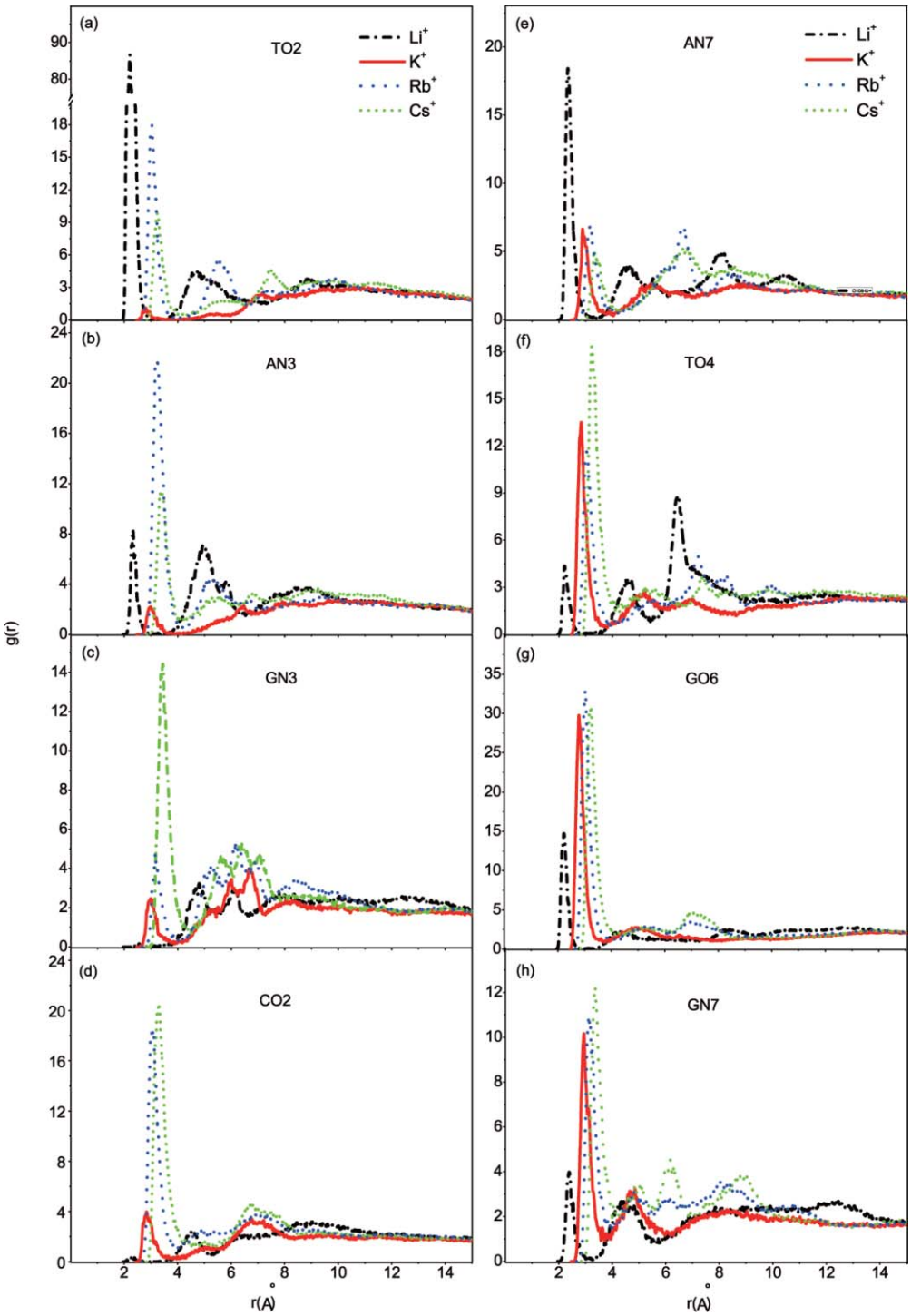

FIG. 10. RDFs between the cations (Li^+, K^+, Rb^+, Cs^+) and (a) O2 of the thymine, (b) N3 of the adenine, (c) N3 of the guanine, (d) O2 of the cytosine, (e) N7 of the adenine, (f) O4 of the thymine, (g) O6 of the guanine, and (h) N7 the of guanine. (a)-(d) give sites in the minor groove and (e)-(h) show sites in the major groove.

interaction with O6 of guanine (GO6) is very strong that the first peak of $g(r)_{K^+}$ exceeds 30 at 3 Å, while the interaction with O4 of thymine (TO4) or N7 of guanine (GN7) is relatively weaker (the first peaks of $g(r)_{K^+-TO4}$ and $g(r)_{K^+-GN7}$ are 13 and 10, respectively). Comparing with Fig. 9(c), MW_{K^+} becomes wide at TpT steps instead of the strongest interaction sites, CpG or GpA steps, similar with the phenomenon discovered in mW_{K^+}. For Rb^+ and Cs^+ ions, the first peaks of $g(r)_{Rb^+}$ and $g(r)_{Cs^+}$ exceed 30 at O6 of guanine (GO6), where MD_{Rb^+} and MD_{Cs^+} become shallower. Except the K^+-DNA interaction, these phenomena indicate that the interactions between ions and base pairs, including direct and water-mediated, strongly influence the shape of the grooves. The heavier ions (Rb^+ and Cs^+ ions) contact with base pairs more closely than the lighter ones (Li^+ ions).

IV. CONCLUSION

In this paper we have presented temperature effects and counterions effects on the structure of a typical B form duplex d (CGCGAATTCGCG). In solvent with Na^+ counterions, when temperature increases from 200 K to 343 K, the DNA changes from the constrained to B form then to the mixed (A-B) structure. At 200 K, the hydrogen-bond is strengthened and Na^+ ions cannot move swiftly in the glass-like solvent. The B-DNA keeps well for the constraint of excessive hydration. When $T = 260$ K, 298 K, and 310 K, the duplex DNA appears flexible B form. At 343 K, the point near to the melting temperature, within the Lennard-Jones like solvent, Na^+ ions show well-distribution around the phosphate groups and intrude into the shell of solvent molecules. The balance comes out between hydrogen-bond with counterions coupling and the B-DNA changes to an intermediate mixed (A-B) structure with helix unwinding and base pairs opening at the peripheries.

For the solvent with different alkali metal counterions, comparing the main chain torsion angle and glycosyl angle at 298 K and 343 K, the sugars appear more flexible and sensitive in the case of Li^+ ions. In Li^+ ions solution, the sugar configuration changes from C2′-*endo* to C1′-*endo* even C3′-*endo* for the close contact between Li^+ ions with free phosphate oxygen atoms. Nevertheless, in the heaviest ions solution (Rb^+ or Cs^+ ions), most of sugars stabilize at C2′-*endo*. As to the counterions effects on the grooves, DNA-K^+ interaction widens mW_{K^+} and MW_{K^+} at ApA steps and TpT steps, respectively, forming the complementation of the width at A-tract. The behaviors of Li^+ ions around base pairs influence the shape of mW_X, mD_X, and MD_X much more than that of heavier ions (Rb^+ and Cs^+). The light ions (Li^+ or Na^+) prefer to distribute around the phosphate groups and influence DNA conformation with ion−O^-(P) interactions while heavy ions (Rb^+ and Cs^+) prefer to reside in the grooves and strongly contact with negative charged atoms forming ion-base pair interactions.

Our simulations show that the DNA structure is sensitive to both temperature and counterions. It seems that B-DNA is influenced by the violent thermal motions more in light ion (Li^+ and Na^+ ions) solutions. Though the heavier ions (Rb^+ and Cs^+ ions) bind tightly to the base pairs at high temperature, the B-DNA keeps stable in the heavier ion solutions. The behaviors of K^+ ions are quite different at high temperature that K^+ ions do not strongly interact with most sites of DNA base pairs. It seems K^+ ions prefer to distribute widely around the duplex DNA instead of coordinating to some special sites. However, appropriate solvent polarity with strong hydration effects is crucial for DNA to hold a special structure for correct biological activity.

ACKNOWLEDGMENTS

The authors thank Ruth Lynden-Bell of Cambridge University for the illuminating discussion. This work was supported by the National Natural Science Foundation of China under Grand No. 11025524, the National Basic Research Program of China under Grant No. 2010CB832903, and the Doctoral Station Foundation of Ministry of Education of China under Grant No. 200800270017 and the Natural Science Foundation of Jiangsu Provincial Universities under Grant No. 10KJB180004.

[1] B. N. Conner, T. Takano, S. Tanaka, K. Itakura, and R. E. Dickerson, Nature (London) **295**, 294 (1982).
[2] A. H. Wang, G. J. Quigley, F. J. Kolpak, J. L. Crawford, J. H. van Boom, G. van der Marel, and A. Rich, Nature (London) **282**, 680 (1979).
[3] D. Watkins, S. Mohan, G. B. Koudelka, and L. D. Williams, J. Mol. Biol. **396**, 1145 (2010).
[4] R. Rohs, S. M. West, A. Sosinsky, P. Liu, R. S. Mann, and B. Honig, Nature (London) **461**, 1248 (2009).
[5] M. J. Arauzo-Bravo and A. Sarai, Nucleic Acids Res. **36**, 376 (2008).
[6] N. Spackova, T. E. Cheatham III, F. Ryjacek, F. Lankas, L. van Meervelt, P. Hobza, and J. Sponer, J. Am. Chem. Soc. **125**, 1759 (2003).
[7] B. Song, D. Li, W. P. Qi, M. Elstner, C. H. Fan, and H. P. Fang, ChemPhysChem. **11**, 585 (2010).
[8] T. Kubar and M. Elstner, J. Phys. Chem. B **112**, 8788 (2008).
[9] R. Tashiro and H. Sugiyama, J. Am. Chem. Soc. **127**, 2094 (2005).
[10] T. E. Haran and U. Mohanty, Q. Rev. Biophys. **42**, 41 (2009).
[11] S. Pal, P. K. Maiti, and B. Bagchi, J. Chem. Phys. **125**, 234903 (2006).
[12] J. Baucom, T. Transue, M. Fuentes-Cabrera, J. M. Krahn, T. A. Darden, and C. Sagui, J. Chem. Phys. **121**, 6998 (2004).
[13] S. Y. Ponomarev, K. M. Thayer, and D. L. Beveridge, Proc. Natl. Acad. Sci. U.S.A. **101**, 14771 (2004).
[14] J. D. Watson and F. H. Crick, Nature (London) **171**, 737 (1953).
[15] F. A. Hays, A. Teegarden, Z. J. R. Jones, M. Harms, D. Raup, J. Watson, E. Cavaliere, and P. S. Ho, Proc. Natl. Acad. Sci. U.S.A. **102**, 7157 (2005).
[16] D. Svozil, J. Kalina, M. Omelka, and B. Schneider, Nucleic Acids Res. **36**, 3690 (2008).
[17] S. Fujii, H. Kono, S. Takenaka, N. Go, and A. Sarai, Nucleic Acids Res. **35**, 6063 (2007).
[18] K. M. Knee, S. B. Dixit, C. E. Aitken, S. Ponomarev, D. L. Beveridge, and I. Mukerji, Biophys. J. **95**, 257 (2008).
[19] R. Lavery, K. Zakrzewska1, D. Beveridge, T. C. Bishop, D. A. Case, T. Cheatham III, S. Dixit, B. Jayaram, F. Lankas, C. Laughton, J. H. Maddocks, A. Michon, R. Osman, M. Orozco, A. Perez, T. Singh, N. Spackova, and J. Sponer, Nucleic Acids Res. **38**, 299 (2010).
[20] A. G. Cherstvy, J. Chem. Phys. **123**, 116101 (2005).
[21] F. J. Solis and M. O. de la Cruz, J. Chem. Phys. **112**, 2030 (2000).
[22] K. M. Knee, S. B. Dixit, C. E. Aitken, S. Ponomarev, D. L. Beveridge, and I. Mukerji, Biophys. J. **95**, 257 (2008).
[23] Y. Q. Li, Q. R. Huang, T. F. Shi, and L. J. An, J. Chem. Phys. **125**, 044902 (2006).
[24] D. Costa, H. D. Burrows, and M. G. Miguel, Langmuir **21**, 10492 (2005).
[25] M. A. Young, B. Jayaram, and D. L. Beveridge, J. Am. Chem. Soc. **119**, 59 (1997).
[26] C. Oostenbrink and W. F. van Gunsteren, Chem. Eur. J. **11**, 4340 (2005).
[27] D. Hamelberg, L. McFail-Isom, L. D. Williams, and W. D. Wilson, J. Am. Chem. Soc. **122**, 10513 (2000).
[28] N. Korolev, A. P. Lyubartsev, A. Laaksonen, and L. Nordenskiold, Nucleic Acids Res. **31**, 5971 (2003).
[29] B. Gu, F. S. Zhang, Z. P. Wang, and H. Y. Zhou, Phys. Rev. Lett. **100**, 088104 (2008).
[30] A. Noy, A. Perez, C. A. Laughton, and M. Orozco, Nucleic Acids Res. **35**, 3330 (2007).
[31] N. Pastor, Biophys. J. **88**, 3262 (2005).
[32] P. L. Freddolino, A. S. Arkhipov, S. B. Larson, A. McPherson, and K. Schultem, Structure **14**, 437 (2006).
[33] J. Precechtelova, P. Novak, M. L. Munzarova, M. Kaupp, and V. Sklenar, J. Am. Chem. Soc. **132**, 17139 (2010).
[34] A. Perez, F. J. Luque, and M. Orozco, J. Am. Chem. Soc. **129**, 14739 (2007).
[35] Y. H. Cheng, N. Korolev, and L. Nordenskiold, Nucleic Acids Res. **34**, 686 (2006).
[36] M. Rueda, S. G. Kalko, F. J. Luque, and M. Orozco, J. Am. Chem. Soc. **125**, 8007 (2003).
[37] A. S. Gerstein, *Molecular Biology Problem Solver: A Laboratory Guide* (Wiley-Liss, New York, 2001).
[38] H. B. Qiu, Y. Inoue, and S. A. Che, Angew. Chem., Int. Ed. **48**, 3069 (2009).

[39]V. A. Bloomfield, D. M. Crothers, and Ignacio Tinoco, *Nucleic Acids: Structures, Properties, and Functions* (University Science Books, Sausalito, 1999).
[40]S. C. Ha, K. Lowenhaupt, A. Rich, Y. G. Kim, and K. K. Kim, Nature (London) **437**, 1183 (2005).
[41]I. Doi, G. Tsuji, K. Kawakami, O. Nakagawa, Y. Taniguchi, and S. Sasaki, Chem. Eur. J. **16**, 11993 (2010).
[42]D. J. Patel, S. A. Kozlowski, L. A. Marky, C. Broka, J. A. Rice, K. Itakura, and K. J. Breslauer, Biochemistry **21**, 428 (1982).
[43]J. Jr. SantaLucia, Proc. Natl. Acad. Sci. U.S.A. **95**, 1460 (1998).
[44]Z. J. Tan and S. J. Chen, Biophys. J. **92**, 3615 (2007).
[45]H. Long, A. Kudlay, and G. C. Schatz, J. Phys. Chem. B **110**, 2918 (2006).
[46]M. Paliy, R. Melnik, and B. A. Shapiro, Phys. Biol. **6**, 046003 (2009).
[47]A. A. Voityuk, J. Phys. Chem. B **113**, 14365 (2009).
[48]T. E. Cheatham III, Curr. Opin. Struct. Biol. **14**, 360 (2004).
[49]Y. von Hansen, R. R. Netz, and M. Hinczewski, J. Chem. Phys. **132**, 135103 (2010).
[50]M. A. Young, G. Ravishanker, and D. L. Beveridge, Biophys. J. **73**, 2313 (1997).
[51]D. Hamelberg, L. MeFail-Isom, L. D. Williams, and W. D. Wilson, J. Am. Chem. Soc. **122**, 10513 (2000).
[52]P. Auffinger and E. Westhof, J. Mol. Biol. **305**, 1057 (2001).
[53]J. W. Toporowski, S. Y. Reddy, and T. C. Bruice, Biophys. Chem. **126**, 132 (2007).
[54]M. Rueda, E. Cubero, C. A. Laughton, and M. Orozco, Biophys. J. **87**, 800 (2004).
[55]A. P. Lyubartsev and A. Laaksonen, J. Biomol. Struct. Dyn. **16**, 579 (1998).
[56]B. I. Schweitzer, T. Mikita, G. W. Kellogg, K. H. Gardner, and G. P. Beardsley, Biochemistry **33**, 11460 (1994).
[57]F. S. Zhang and R. M. Lynden-Bell, Phy. Rev. E **71**, 021502 (2005).
[58]R. M. Lynden-Bell and P. G. Debenedetti, J. Phys. Chem. B **109**, 6527 (2005).
[59]K. Toukan and A. Rahman, Phys. Rev. B **31**, 2643 (1985).
[60]W. D. Cornell, P. Cieplak, C. I. Bayly, I. Gould, K. M. Merz, Jr, D. M. Ferguson, D. C. Spellmeyer, T. Fox, J. W. Caldwell, and P. A. Kollman, J. Am. Chem. Soc. **117**, 5179 (1995).
[61]A. D. Mackerell, J. Comp. Chem. **25**, 1584 (2004).
[62]A. P. Lyubartsev and A. Laaksonen, Comput. Phys. Commun. **128**, 565 (2000).
[63]R. Lohikoski, J. Timonen, and A. Laaksonen, Chem. Phys. Lett. **427**, 23 (2005).
[64]M. Tuckerman and B. J. Berne, J. Chem. Phys. **97**, 1989 (1992).
[65]D. Fincham, Mol. Simul. **13**, 1 (1994).
[66]E. Stofer and R. Lavery, Biopolymers **34**, 337 (1994).
[67]R. E. Dickerson, Nucleic Acids Res. **17**, 1797 (1989).
[68]J. R. Errington and P. G. Debenedetti, Nature (London) **409**, 318 (2001).
[69]M. A. Young, B. Jayaram, and D. L. Beveridge, J. Phys. Chem. B **102**, 7666 (1998).
[70]W. Saenger, *Principles of Nucleic Acid Structure* (Springer-Verlag, New York, 1984).
[71]J. M. Vargason, K. Henderson, and P. S. Ho, Proc. Natl. Acad. Sci. U.S.A. **98**, 7265 (2001).
[72]D. Jose and D. Porschke, J. Am. Chem. Soc. **127**, 16120 (2005).
[73]M. P. Allen and D. J. Tildesley, *Computer Simulation of Liquids* (Oxford University Press, Oxford, 1987).
[74]T. Rules, Eur. J. Biochem. **17**, 193 (1970).
[75]R. E. Dickerson, H. R. Drew, B. N. Conner, R. M. Wing, A. V. Fratini, and M. L. Kopka, Science **216**, 475 (1982).
[76]R. E. Dickerson and H. L. Ng, Proc. Natl. Acad. Sci. U.S.A. **98**, 6986 (2001).
[77]H. R. Drew, R. M. Wing, T. Takano, C. Broka, S. Tanake, K. Itakura, and R. E. Dickerson, Proc. Natl. Acad. Sci. U.S.A. **78**, 2179 (1981).
[78]P. Varnai and K. Zakrzewska, Nucleic Acids Res. **32**, 4269 (2004).
[79]Q. Dong, E. Stellwagen, and N. C. Stellwagen, Biochemistry **48**, 1047 (2009).
[80]D. Hamelberg, L. D. Williams, and W. D. Wilson, J. Am. Chem. Soc. **123**, 7745 (2001).